Paleoenvironment reconstruction through paleosols in the Ebro Foreland Basin System, Spain: Evidence of global climate change

Kathryn Stalker
Senior Integrative Exercise
March 9, 2005

Submitted in partial fulfillment of the requirements for a Bachelor of Arts degree
from Carleton College, Northfield, Minnesota

Table of Contents

Paleoenvironment reconstruction through paleosols in the Ebro Foreland Basin System, Spain: Evidence of global climate change

Kathryn Stalker
Senior Integrative Exercise
March 9, 2005

Advisors:
Dave Barbeau, University of South Carolina
Bereket Haileab, Carleton College

Abstract
Paleosols from the bottom of the Ebro Foreland Basin stratigraphic sequence are used in a paleoenvironmental reconstruction through X-Ray Fluorescence spectrometry geochemical analysis. It is believed that the paleosols developed on or very near the forebulge of the foreland basin. The paleosol data may indicate a climatic shift from humid and tropical to an arid setting to explain the change in composition without evidence of an alteration in source material. The climate shift is represented by the bottom of the section consisting of humid environment vertisols and tufa freshwater carbonates, transitioning to increased aridness in the area, characterized by calcisol and gypsisol paleosols. The climate change is likely to have occurred across either the Paleocene-Eocene thermal maximum, or the Eocene-Oligocene glaciation.

Key words: paleosol, forebulge, Ebro Basin, climate change

Introduction:

For this project, section data and paleosol (ancient soil) samples were collected from the southeastern part of the Ebro Basin, which has been interpreted to have formed on the forebulge of a flexural wave created by the dominant Pyrenean load and the lesser Catalan Coastal Range load (Fig. 1; Fig. 2) (Barbeau, 2003). The paleosols are used to investigate the forebulge hypothesis and to better understand their paleoenvironment. The local geologic map misrepresents the paleosols as Cretaceous grey and white carbonates; this mistake emphasizes the unconstrained nature of basin's development in both composition and timing (Catalunya, 2003). Previous work on the paleosols has been limited to stratigraphic measurements (Barbeau, 2003; Barbeau et al., 2005). Paleosols are located at the bottom of the foreland basin section and provide insight into the timing and environment in which the foreland basin system developed.

At the very bottom of the paleosol formation is a vertisol, using Mack et al.'s (1993) definition of a vertisol characterized by its homogeneity which arises through the process of swelling and shrinking clays. Above it is a freshwater limestone, also known as tufa. Next in the stratigraphic sequence is the second paleosol, characterized by its calcium rich nodules. It is called a calcisol, using the definition encompassing any paleosol in which high $CaCO_3$ is the prominent pedogenic feature (Mack et al., 1993). Up section is a gypsum rich soil. The sulfated pedogenic accumulations could possibly have been re-crystallized from elsewhere, confusing the primary or secondary nature of the gypsiferous soil (Meyer, 1997). It appears the gypsum is pedogenic because of the massive rather than veined appearance, so its paleosol classification is gypsisol (Mack et al., 1993). The sequence is topped off by lacustrine marl.

A.

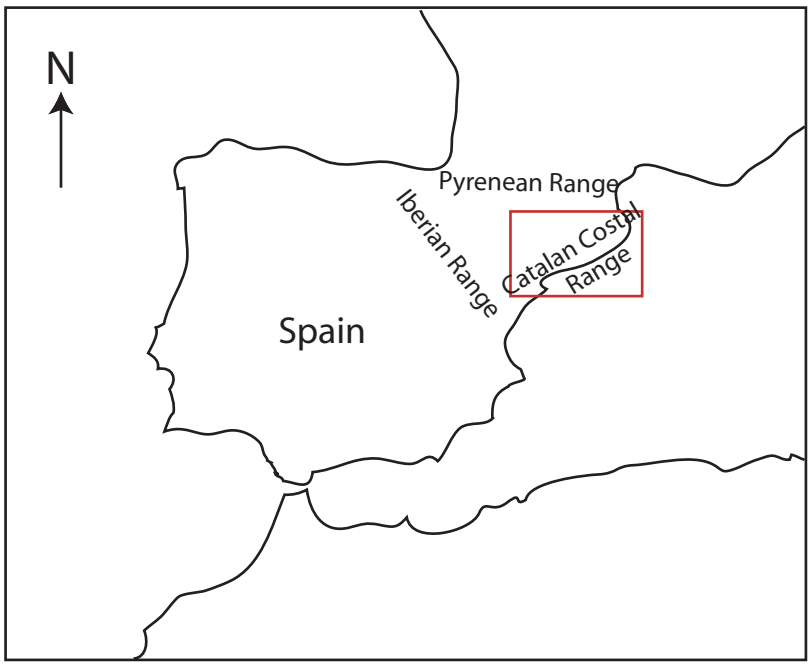

B.

Figure 1: A. Line drawing of the Iberian Peninsula, the Ebro Basin is contained within the three mountain ranges. Close-up shown below is outlined in a red box. B. LANDSET image of the eastern Ebro Basin. The Pyrenees lie to the north, the Iberian Range is off the map to the west and is connected to the Catalan Coastal Range by the "linking zone". Paleosol field area is denoted with yellow star near the town of Horta de San Joan.

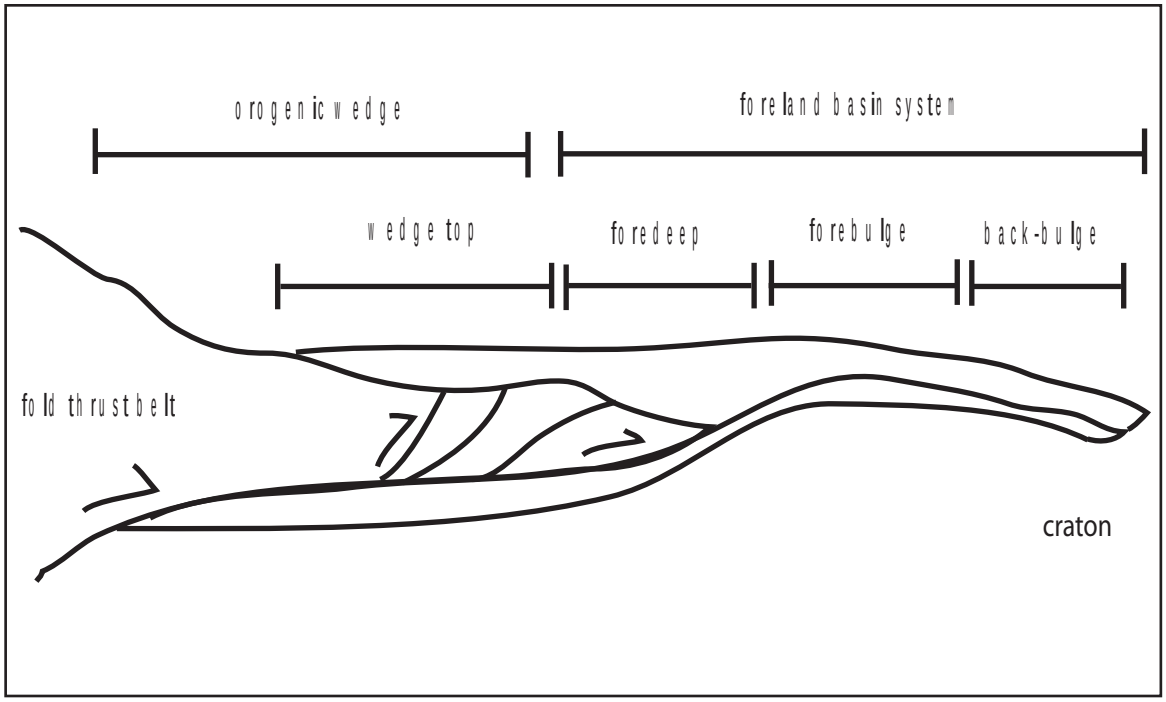

Figure 2: Generalized foreland basin system. Adapted from Decelles and Giles (1996). The Pyrenean Mountains are believed to be the major lithospheric load in the Ebro Basin. This loading creates flexure of the lithosphere, causing a forebulge in the basin. The paleosols are hypothesized to form on top of the forebulge.

A combination of field measurements, observations, and X-Ray Fluorescence spectrometry (XRF) whole rock geochemistry data was used to analyze the samples. XRF spectrometry was chosen because it is resistant to alteration upon diagenesis, as apposed to X-Ray Diffraction (XRD), which is also used to analyze modern and ancient soils for compositional characteristics (Retallack, 1997). Results indicate that the paleosols record a change from humid tropical environment to a more arid climatic setting. This transition could coincide with the Paleocene-Eocene or Eocene-Oligocene boundaries.

Geologic Setting

The Ebro Basin in Spain is a triangular depression with the Pyrenees lying to the North, Catalan Coastal Range to the southeast, and the Iberian Range to the southwest (Fig. 1). The collision of Europe and the Iberian microcontinent in the Cretaceous caused the formation of the Pyrenean, Iberian, and Catalan Coastal ranges (Barbeau, 2003). This mountain building continued from the uppermost Cretaceous until the lower Eocene, with northwest movement of the Iberian Plate generating the Pyrenees and the other two smaller mountain ranges (Guimera, 1984).

The Pyrenees are believed to be the major control of the basin, creating the foreland basin depression by providing a tectonic load, resulting in a lithospheric flexure (Fig. 2) (Barbera et al., 2001). Sedimentation from all three ranges is evident in the basin (Barbera et al., 2001). Estimates of Ebro Basin sedimentation are believed to have begun in the Paleocene or Eocene (Barbeau et al., 2005). The Catalan Coastal Range is made of Jurassic-Triassic carbonates and dolomites, which are believed to be the major source material for the basin fill at the paleosol field site (Fig. 3) (Catalunya, 2003). The Ebro

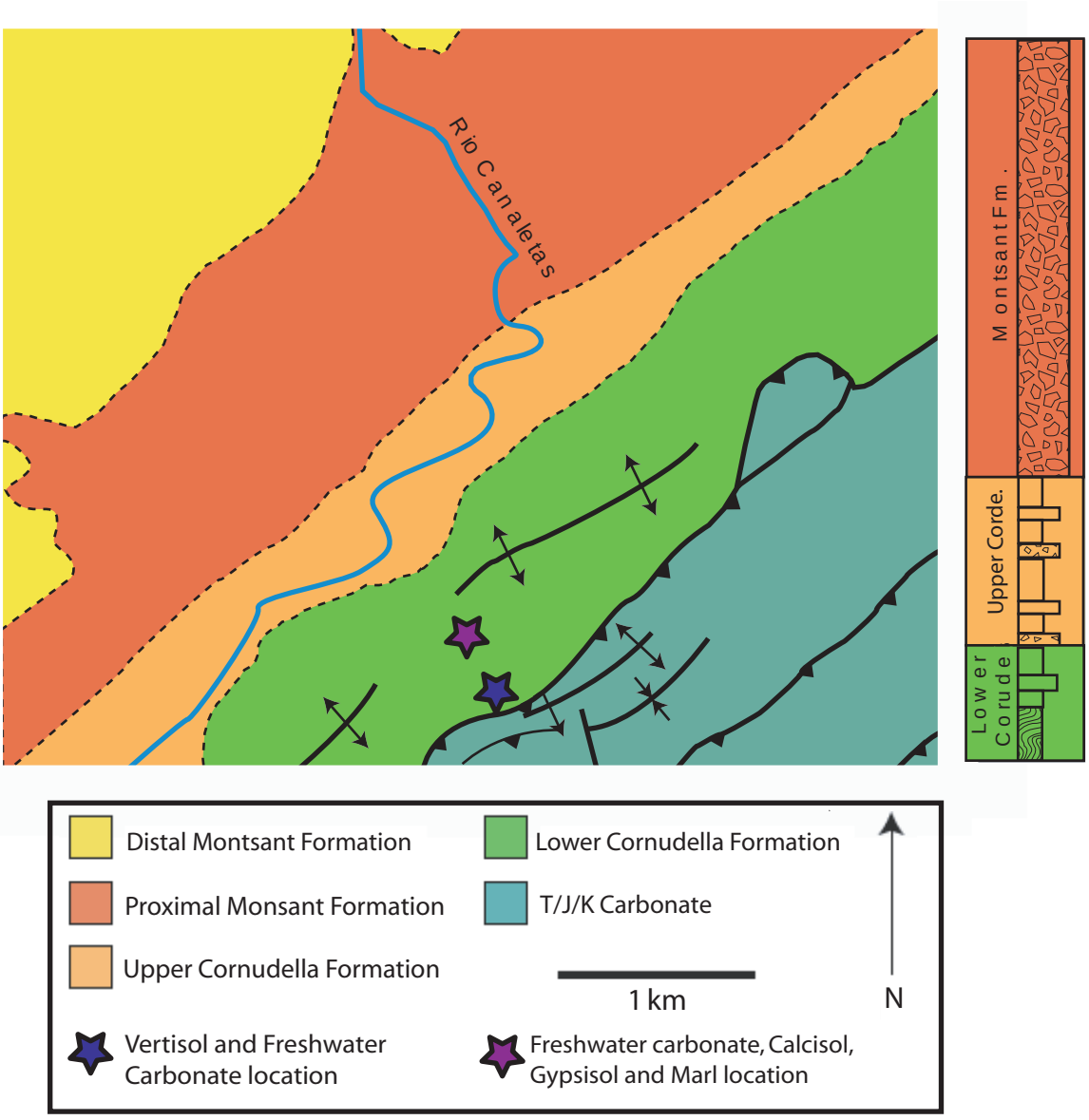

Figure 3: A simplified geologic map of the study area modified from Swanson-Hysell (2005). The Lower Cornudella formation is described as a forebulge facies made of paleosols, lacustrine marls and fluvial mudstones (Barbeau et al. 2005). The Upper Cornudella is fluvial sandstones and terrestrial mudstones; the Montsant formation is alluvial fan and fluvial megafan conglomerates (Barbeau et al. 2005). The stratigraphic column shows the vertical proportions of the formations. The paleosol locations are denoted by stars and correlated to eachother through freshwater carbonates.

Basin is backfilled with up to 3km of a terrestrial sedimentary succession occurring through the middle Miocene (Barbeau, 2003). The paleosol and marl sequence is covered by basin fill of fluvial mudstone and sandstone transitioning into an alluvial fan conglomerate (Fig. 3) (Barbeau, 2003). The sediments deposited in growth structures above the paleosol formation were derived from thrust sheets of carbonate-bearing material that hold up the modern Catalan Coastal Range (Barbeau, 2003).

Paleomagnetic data suggests that during the Paleocene to early Eocene, the Iberian peninsula occupied the area where the Sahara lies today, with the Basque region (currently north of Catalan) standing at about 35ºN (Schmitz et al., 2001). The southern part of the Ebro Basin currently resides at 41°N (Catalunya, 2003).

Methods

The paleosol succession was located with the help of David Barbeau. The paleosols were measured using a jacob staff to approximate the small scale tectonic folding that caused the dip of the beds. The entire stratigraphic section was discontinuous due to small scale regional folding, so the body was measured in two sections about 300 meters from each other laterally (Fig. 3; Fig. 4). After the paleosols were measured, clean faces were exposed 20 cm into the semi-lithified sections. Samples were taken from the trenched exposures to avoid weathered surfaces and the development of modern soil on top of the paleosols. Part of the calcisol paleosol was poorly exposed due to vegetation cover and therefore hard to sample, so samples were only collected from the upper half of the calcisol section, which was better exposed in a road cut. Samples were hammered out of the trenches at recorded intervals with steel rock

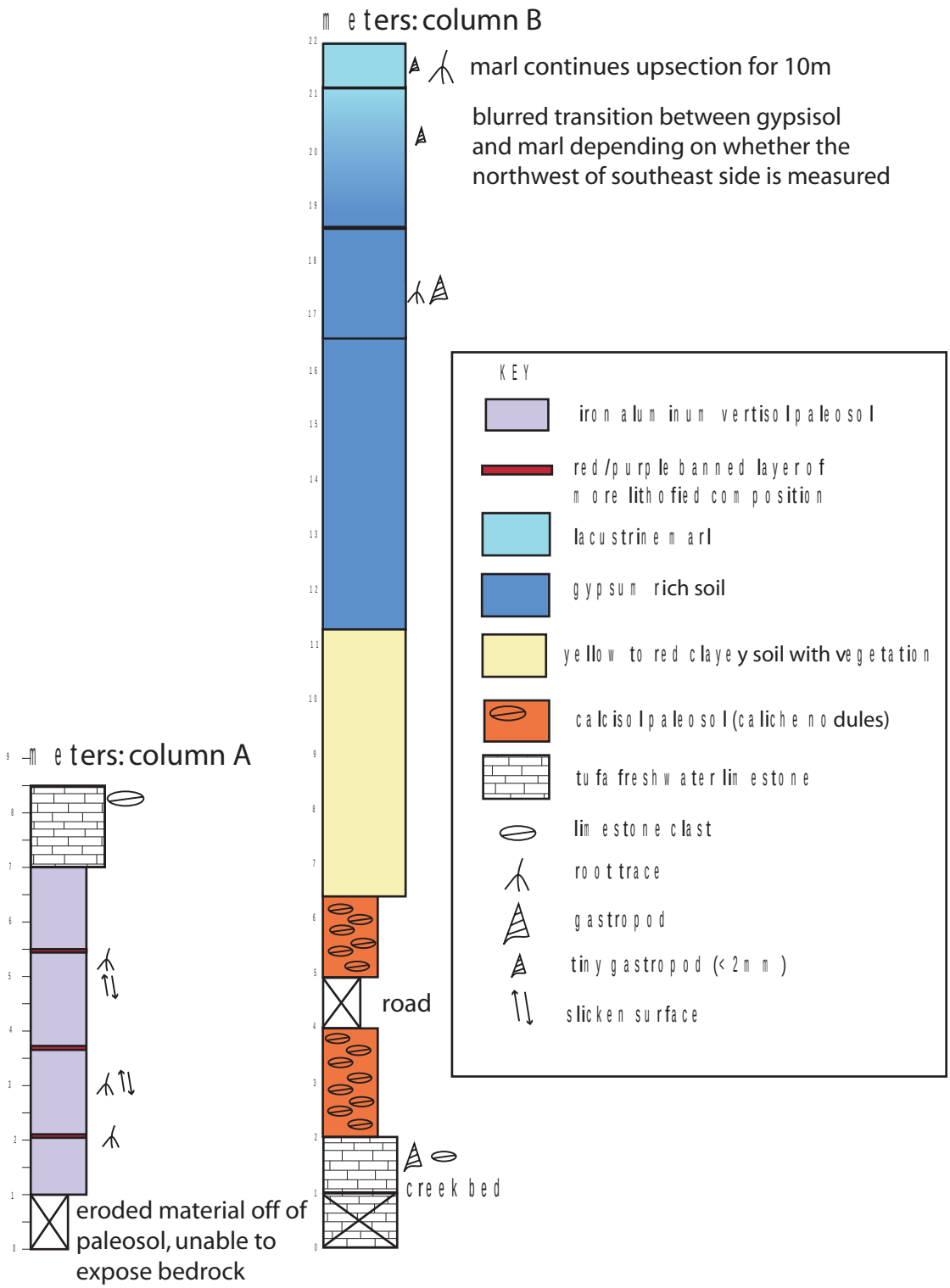

Figure 4: Stratigraphic columns. The left column is the lower part of the sequence (column A); the right represents the upper section (column B). Columns are correlated by freshwater tufa carbonates. Due to small scale regional folding, carbonates were separated by approximately 300 meters in distance. The marl continues above column B for approximately 10 additional meters.

hammers and placed in clean plastic film canisters. Two or three samples were collected at each of the sample locations.

At Carleton College, the paleosols were crushed using the Jaw Crusher and powdered with agate balls within agate cups. All the samples for each stratigraphic location were crushed together for homogeneity. Ten samples, five from the vertisol and five from the calcisol, were dried, sieved, and analyzed by the XRF at Activation Laboratories-Skyline in Tucson, AZ. Samples of a tufa freshwater limestone and a calcisol limestone nodule were sent to Spectrum Petrographics (Winston, OR) for thin section preparation.

Field Observations

The section begins with a six meter high red, purple and white colored paleosol (Fig. 5). It was moderately lithified, sometimes with very hard stones of deep red to purple colored rock. The composition dissolves into 95% clay with some sand grains. There are three levels of more resistant red lithified rock (Fig 5A). The harder layers had locally preserved slickensides scattered infrequently throughout. These layers created horizons, but were not always preserved further into the outcrop. The red, purple and white often appeared molted together in unweathered surfaces. The contrasting shades of clay also highlight features such as root casts, the only biological feature of the paleosol still preserved. The root casts often occurred in the white clay, and were filled in with pink to red colored clay (Fig. 5B). Root casts are infrequent in the vertisol due to the turbation of the material from clays hydrating and dehydrating.

Figure 5: (A) Overview of vertisol, 1.5 meter jacob staff for scale. Yellow line marks boundary between vertisol and fresh water carbonate. (B) Root trace outlined in ink, pen for scale. Found approximately 3m from bottom of section. (C) Dugout trench. Note the more blocky peds and molted colors in the unexposed section.; 1.5 meter jacob staff for scale.

On top of the red and white paleosol sat a 1.5 meter limestone with a poorly defined structure (Fig. 6). The weathered part of the limestone had small (1-3cm), bulbous features covering it. When broken apart, a variety of shades of yellow and orange mixed in swirls, and clasts of limestone were held within. Further up the hillside, the limestone body appears with other rounded to subangular limestone clasts contained within it. No bedding features exist in the limestone. This layer is covered by thick vegetation and man-made terraces.

The next exposure, approximately 300m away, begins with a streambed, which flows on top of limestone (Fig 7). The limestone contains gastropod shells (1-2cm), laminae and clasts of limestone with a semi-rounded appearance (Fig. 7B).
Rising out of this streambed is the second section of paleosol, standing 3.85 meters tall (Fig. 8). It is composed of red-brown colored clays as a matrix containing large 2-15cm strongly lithified nodules of limestone (Fig. 8B). The nodules are a light taupe color with lots of spherical discolorations when broken open, in deep red-brown colors. The clasts are plentiful throughout the body of paleosol, rather than isolated in layers.

On top of the paleosol with calcite nodules is a layer of poorly developed, clay-rich soil varying from between yellow to red in color. In the clay-rich soil, large bodies of gypsum (approximately 10m continuously vertical) appear and the soil becomes only red in color (Fig. 9). The soil throughout is poorly lithified. Above the massive gypsum, the soil has what appears to be large scale root casts (30cm in length). The sequence is topped with marls, which continue approximately 10 meters above the paleosol sequence. The lowest marl has small fossils and root casts. The marls are white in color and the material is very carbonate heavy, as acid tests lead to rapid dissolution.

Figure 6: Lower tufa freshwater carbonate (from Figure 4, column A). (A) Overview of lower tufa section stands 1.5m vertical, resting on top of vertisol. (B) Close-up of limestone, pen for scale.

Figure 7: Tufa freshwater limestone exploited as creek bed (Figure 4 column B), bottom of the upper section. (A) Carbonate clasts and molting within limestone., pen for scale. (B) Gastropod shell in limestone, carbonate clasts, laminations within the matrix, pen for scale.

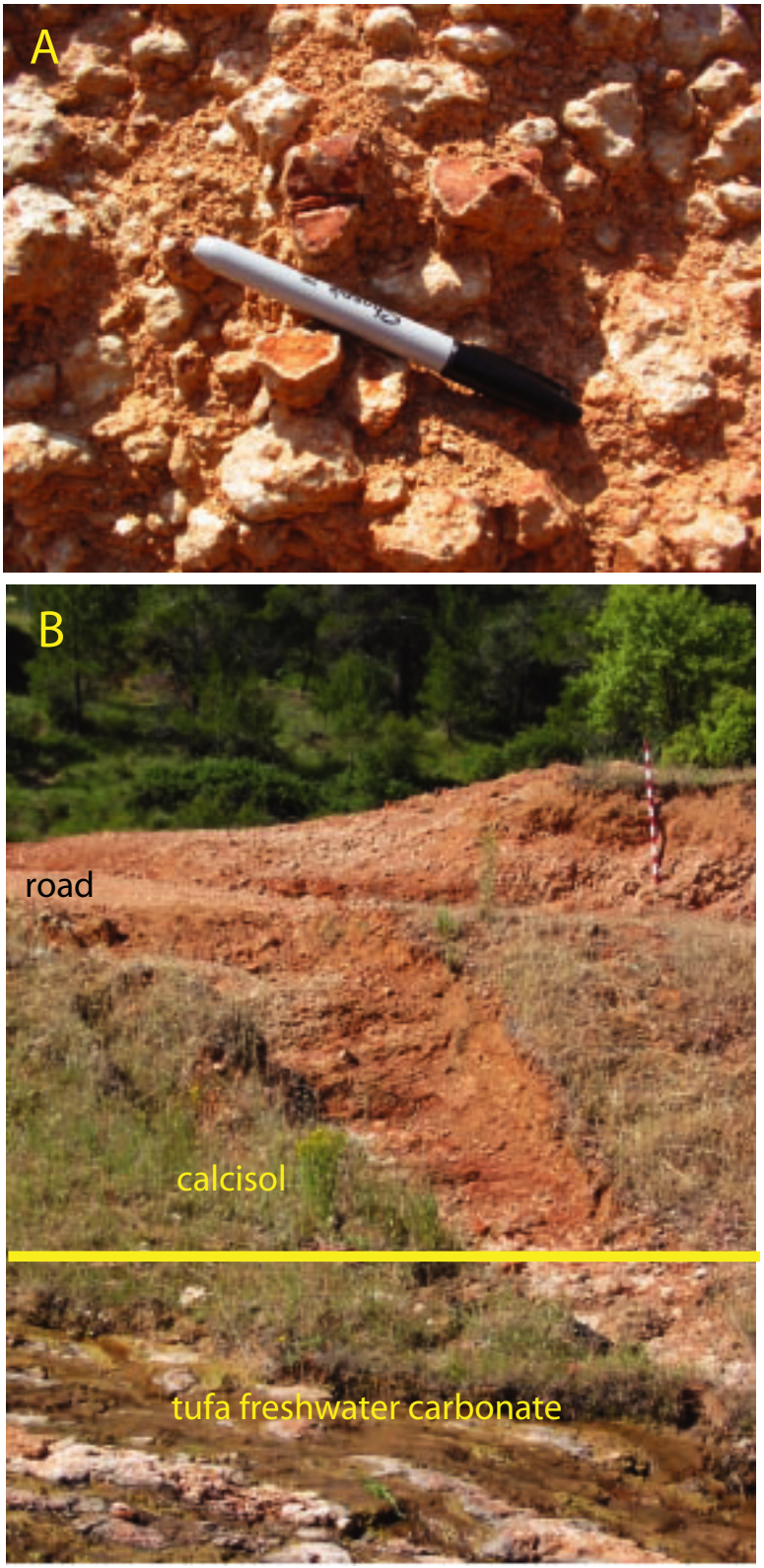

Figure 8: Calcisol paleosol. (A) Caliche nodules within clay-rich matrix. Nodules closest to the pen are broken open to reveal reddish interior color. (B) Creek bed of freshwater limestone transitioning into calcisol paleosol. There is an inaccessible section of approximately one meter where the road cuts through paleosol. Jacob staff for scale.

Figure 9: Gypsisol above clay rich soil (ranging in color from yellow to red) and lacustrine marl (top of section; white). Southeastern side of hill slope. Foreground shows massive gypsum with blade like features, transitioning into red soil which has root traces, capped by white marl. On the northwest side the formation is less thick and the soil more yellow in color.

Thin Section Analysis

The freshwater limestone, sampled from the lower section, is dominated by quartz grains held within calcitic and miciritic cement (Fig. 10). The brown oxides in Figure 10A could be filled in root hairs. Spherical features made of calcite appear to be some type of remnant biogenic feature, such as a root or ostracod, or peloids of carbonate washing away from an existing distant carbonate alluvial fan (Fig. 10B). The peloid hypothesis could explain why both fine and course grains are held in the center. No laminations are present, which would be indicative of microbial communities.

The calcisol nodules are calcite and micirite with some scattered quartz grains (Fig. 11). The thin section is dominated by spherical remnants of old roots, filled in with heavy calcitic cement and micirite accumulated on the edges.

Data

Whole rock XRF data gives a silicon dioxide range between 52.5% and 76.9% for the vertisol, and between 14.6% and 22.1% for the calcisol (Table 1). The Al_2O_3 whole rock percentages range between 6.6 and 27.2 for the vertisols, and 3.8 and 7.3 for the calcisol (Table 1). The CaO percentages for the vertisol range between 0.16 and 0.35 in the vertisol and 33.1 and 40.1 for the calcisol (Table 1). The vertisol ranges between 5.2% and 10.9% Fe_2O_3, while the calcisol has values of 1.8% and 2.5% for the iron oxide (Table 1). The amount of vertisol Loss on Ignition (LOI) ranges from 3.7% and 11.0%, while the calcisol ranges from 33.1% and 36.4% (Table 1). Potassium oxide weight percentages range from 0.01 to 0.54 for the vertisol, 0.43 to 0.76 for the calcisol. The TiO_2 ranges between 0.48% and 1.12% for the vertisol, 0.23% to 0.36% for the calcisol.

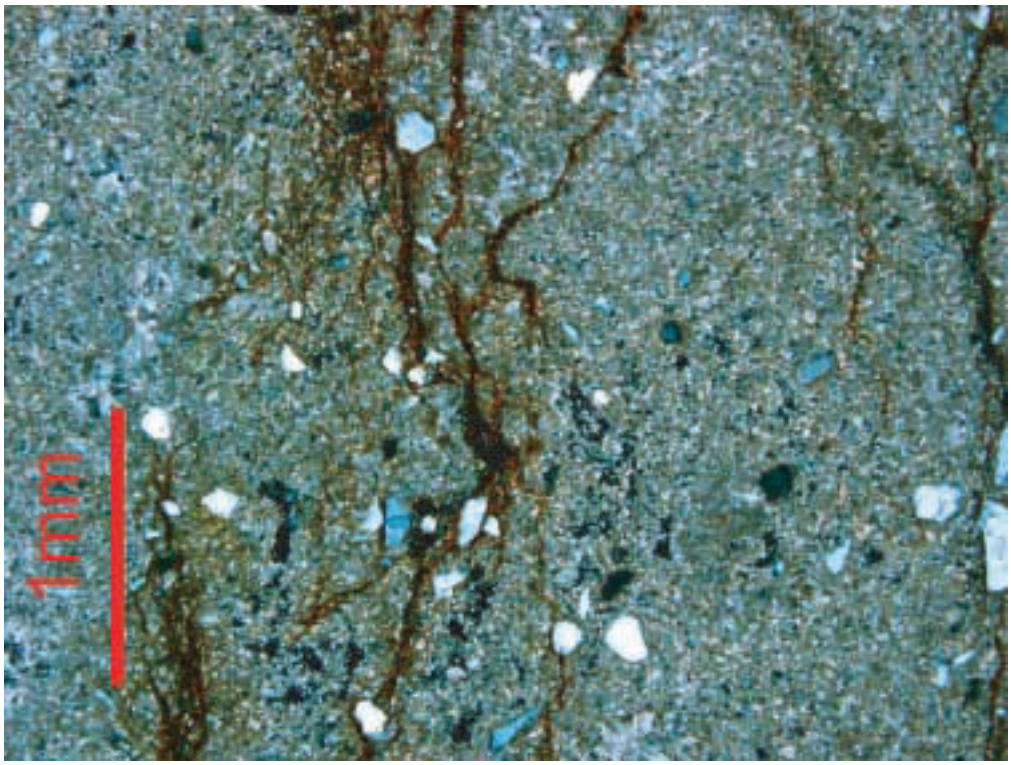

(A) Cross polarized light, grains of quartz in miciritic matrix. Hairs of brown semi-opaque oxides.

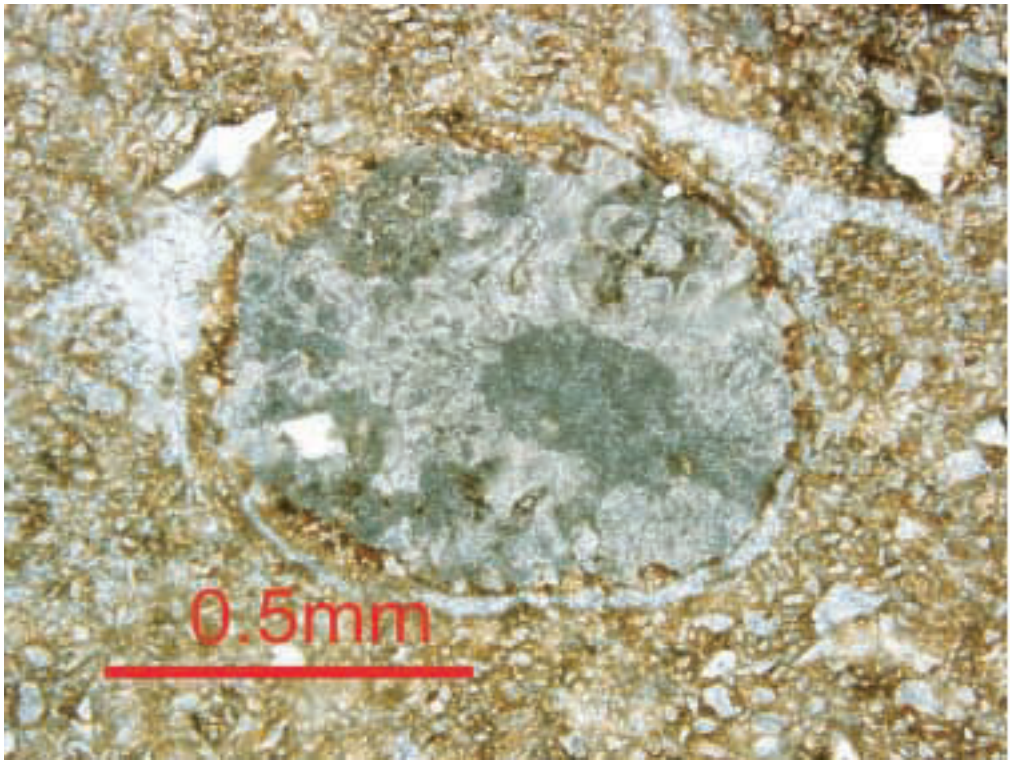

(B) Plane polarized light, cryptic biogenic remnant or terrestrial peloid from source area, filled with calcite.

Figure 10: Tufa freshwater limestone thin section, from lower section.

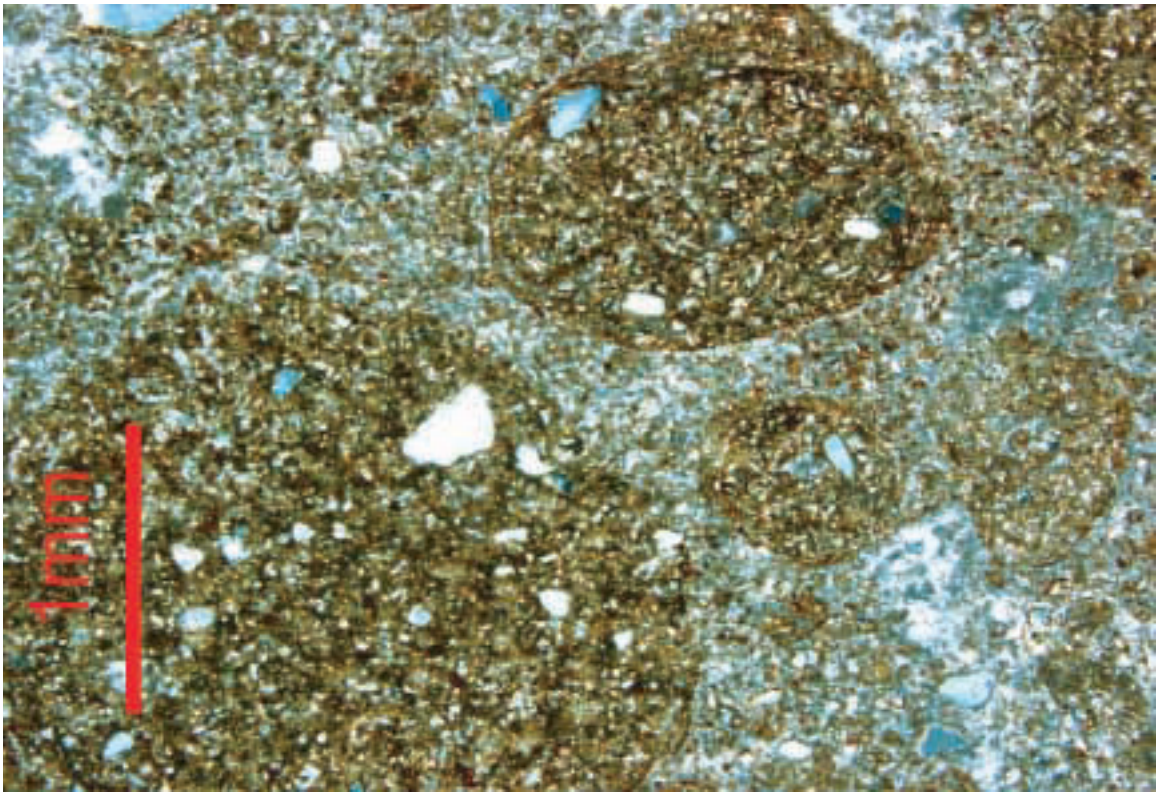

(A) Cross polarized light, rhizolites formed in micirite, larger grains of quartz

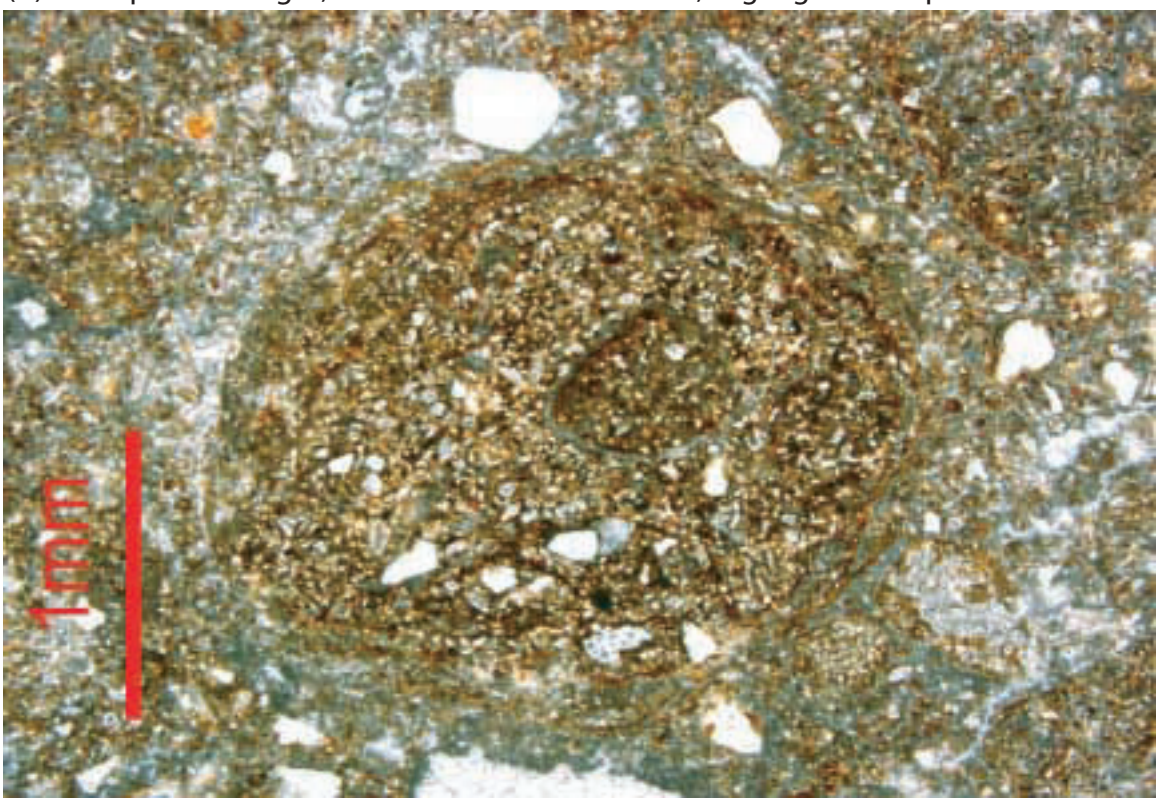

(B) Plane polarized light, calcitic cement outlining root traces.

Figure 11: Caliche nodule from calcisol paleosol.

SAMPLE	Al_2O_3 (%)	CaO (%)	Cr_2O_3 (%)	Fe_2O_3 (%)	K_2O (%)	MgO (%)	MnO (%)	Na_2O (%)	P_2O_5 (%)	SiO_2 (%)	TiO_2 (%)	LOI (%)	Total (%)
VER: 2.8meter	12.86	0.16	0.04	5.20	0.15	0.13	0.007	0.08	0.09	74.46	1.12	5.82	100.12
VER: 3.7meter	6.60	0.35	0.01	10.93	0.10	0.07	0.005	0.05	0.04	76.89	0.48	3.66	99.18
VER: 4.3meter	16.44	0.16	0.01	10.27	0.11	0.14	0.006	0.07	0.04	64.60	0.96	7.42	100.23
VER: 5.5meter	27.19	0.27	0.02	7.47	0.54	0.19	0.009	0.12	0.19	52.51	0.88	10.96	100.35
VER: 6.3meter	9.99	0.26	0.01	8.54	0.32	0.12	0.006	0.08	0.03	75.34	0.77	4.66	100.12
CAL: 5.1meter	4.79	34.42	-0.01	2.37	0.55	2.31	0.039	0.05	0.02	22.12	0.31	33.13	100.10
CAL: 5.4meter (1)	3.87	39.64	-0.01	1.94	0.43	1.86	0.056	0.05	0.02	16.31	0.23	35.82	100.22
CAL: 5.4meter (2)	3.85	39.70	-0.01	1.94	0.43	1.88	0.055	0.05	0.02	16.33	0.23	35.82	100.30
CAL: 5.8meter	4.59	38.81	-0.01	1.83	0.53	1.76	0.052	0.05	0.02	17.06	0.26	35.30	100.25
CAL: 6.1meter	4.30	40.18	-0.01	2.30	0.44	1.50	0.056	0.04	0.02	14.63	0.24	36.38	100.07
CAL: 6.5meter	7.32	33.05	-0.01	2.48	0.76	1.90	0.058	0.09	0.02	21.16	0.36	33.10	100.29

Table 1: X-Ray Fluorescence Data from the vertisol (VER) and calcisol (CAL) paleosols. Data displays total weight percentages of the oxides. The meter level is measured from bottom of stratigraphic sections (Fig. 4). The sample from CAL 5.4meter was run twice to compare the accuracy of the method.

Results

Vertisol

Vertisols are characterized as weathered soils in which the clays within shrink and swell (Buol et al., 2003). Vertisols are easily developed from limestone and alluvium; these materials are characteristic of the parent material in the Ebro Basin locality (Buol et al., 2003). The vertisol has zones of red color horizons; these regions typify areas with more precipitation, as the more soluble elements wash out of the soil leaving iron and aluminum (Bestland et al., 1996). The molted appearance of the vertisol is typical of leaching under reducing conditions (Bestland et al., 1996).

Freshwater carbonate

The limestone is a microbial freshwater carbonate tufa with a sandy composition, as evidenced in thin section. It can be difficult to identify tufa because its characteristic porosity diminishes upon diagenesis (Meyer, 1997). The limestone most likely formed in shallow water, as this is characteristic of the tufa composition and possible root hairs found in thin section. Clasts of limestone were consumed in the carbonate deposition surrounding them, which makes this formation unlikely to have developed as a soil. It is believed that the limestone in the upper section is from the same body as the lower limestone because the clast heavy compositions appear similar; however, further investigation is needed for confirmation.

Due to it lack of biologic features, such as laminations, occurring in the thin section, tufa formation in the Ebro Basin likely occurred as precipitation from carbonate supersaturated waters (Glover and Robertson, 2003). The intraclasts are characteristic of shallow water lacustrine or paludal environments, which would have slower deposition

than agitated environments (Glover and Robertson, 2003). The nearby Catalan Coastal Range provides a ready source for the clasts found in outcrop. Inorganic precipitation of freshwater carbonates occurs frequently in turbulent flows, while biomediation is predominate in sluggish waters (Pedley et al., 1996). The thin section contains a few spherical features, which could be remnants of original organic matter or sourced off of the alluvial fan of surrounding mountain ranges.

Both the limestone and calcisol thin sections have grains of quartz. While the nearby limestone mountains are the likely a major supplier of material, the source of quartz is likely windblown, either from quartz grains within the limestone mountains or from further sources (Delgado et al., 2003). Delgado et al. (2003) report that Saharan aeolian dust brings quartz to Spain, and that very fine sand can easily cover moderate 200km distances. Desertification in the Sahara would not have been similar to present day analog during tufa and paleosol development, but the warm periods of the Mesozoic, Paleocene and Eocene are all associated with aridness on the North African craton. West and North Africa were associated with warmth and increased aridity during the late Paleocene (Bolle et al., 2000).

Calcisol

The calcisol is dominated by calcitic nodules, which are remains of root tubules (Hubert, 1977). These are also known as caliches, which form as clacitic concretions around pedotubules in nodular limestone (Hubert, 1977). The tubuals within the calcisol nodules are spherical and linear; this environment of deposition is vegetation mediated through rhizolites, rather than micro-organism mediated. Calcisols typically form on top

of limestone or when an aeolian environment transports an adequate amount of Ca^{2+} cations (Meyer, 1997).

Gypsisol

The gypsisol is a clay rich soil with massive bodies of gypsum. The Ebro Basin has a large number of Tertiary gypsum deposits formed after marine transgressions during the tectonic development of the basin (Elorza and Santolalla, 1998). Poorly constrained marine transgressions continued through the Paleocene-Eocene (Elorza and Santolalla, 1998). It seems unlikely that a marine transgression would occur at this site, as it is a terrestrial sequence, and near or on a topographic high (due to the flexure of the lithosphere creating a forebulge). The gypsum in the soil appears to be an original feature of the paleosol, whose development occurred separately from the marine evaporates. However, the presence of evaporites in the general basin provides a large source of sulphides to facilitate gypsisol development. The field observations do not show evidence that the gypsum formation occurred underwater, as it is interspersed with clay-rich soil. Furthermore, no marine limestone or other marine indicator is present in the soil sequence. Once the uplift of the Ebro Basin was completed, alluvial fans and shallow lacustrine environments occurred, with evaporitic lakes and carbonate sedimentation (Elorza and Santolalla, 1998). This type of environment would allow for the formation of gypsisols in terrestrial environments.

Marl

Marl is lacustrine. It is a white body of calcareous fine grained chalk and frequent microfossils characteristic of terrestrial deposition. It is constrained on soils and below fluvial facies, further representative of its lacustrine deposition.

Vertisol XRF

The whole rock geochemistry values for the vertisol demonstrate diagenesis had a more prominent effect higher in the section. Potassium accumulates upon diagenesis (Driese et al., 2000). The vertisol shows that potassium increased three to five fold in the uppermost data points (Table 1). Titanium is considered an immobile index element in paleosols (Driese et al., 2000). The titanium values are approximately twice as large for the vertisol selection in comparison to the calcisol, which could be a proxy for a greater time of development for the vertisol.

The vertisol has particularly high Fe values, especially if its parent material is assumed to be limestone. The source of iron is likely to be Saharan dust windblown into the system (Delgado et al., 2003). The buildup of weathering products such as oxides; especially aluminum, titanium and manganese, are an indicator of humid climate, either warm or cold (Bestland et al., 1996). The base loss shows a buildup of insoluble products with respect to soluble materials (Ca^{2+}, Mg^{2+}, Na^{+}, K^{+}) liberated by weathering through aqueous movement (Fig. 12) (Retallack, 1997). No prominent trend of base loss is evident throughout the vertisol, most likely because the overall molted appearance allows for the hydration and

dehydration of the clay composition, mixing up any previous segregation of materials. Base loss for the vertisol is approximately 25 weight percent, while the calcisol values are around 1 weight percent.

Clayeyness is a gauge of clay formation and of podzolization (Fig. 12) (Retallack, 1997). The vertisol data show a trend of increased clay-richness and acidicness up section, however, the last data point stands out as an anomaly to this trend. Data from the

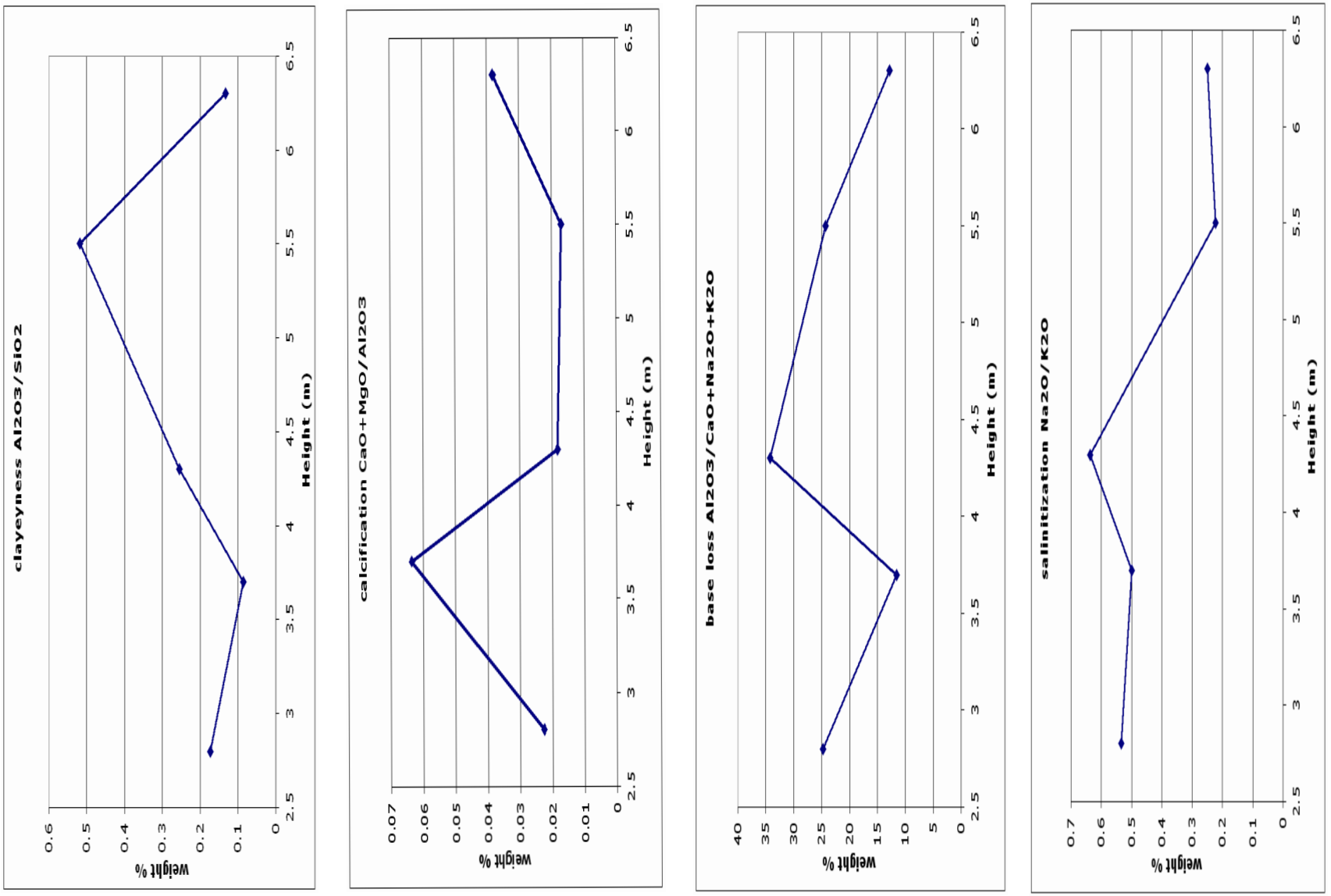

Figure 12: Vertisol data. Relationships from Retallack (1997), showing clayeyness (Al_2O_3/SiO_2), calcification ($CaO+MgO/Al_2O_3$), base loss ($Al_2O_3/CaO+Na_2O+K_2O$) and salinitization (Na_2O/K_2O).

vertisol shows an overall decrease in salinitization through the section. This trend reinforces the hypothesis that the limestone directly above it in the stratigraphic section is freshwater.

Replacement of CaO by MgO can be an indicator of dolomitization (Driese et al., 2000). The disproportionately high ratio of CaO to MgO at 3.7m could mean that dolomitization is not a prominent feature at that level, but that process was active in the rest of the vertisol (Fig. 12). Overall, calcification shows little trend in the vertisol, and the most significant thing it conveys is the near loss of Ca^{2+} cations in a surrounding carbonate rich environment. The values for calcification are very small because the variation is the result of small concentrations of calcium and magnesium within the paleosol.

Calcisol XRF

The Loss On Ignition (LOI) numbers for the calcisol data are similar to the amount of CaO recovered, therefore indicating that most of the LOI was CO_2 from the combustion of $CaCO_3$. The percentage of $CaCO_3$ ranges between 66% and 77% (CaO+LOI) (Table 1). With the $CaCO_3$ factored out and the oxide values recalculated, the amounts of SiO_2, Fe_2O_3, Al_2O_3 and TiO_2 recalculate within similar ranges as the vertisol. For the vertisol, the Al_2O_3 ranges between 6.6%-27.2%, without the $CaCO_3$ in the calcisol, the Al_2O_3 range is 14.7%-21.6%. Similarly for iron oxide, the calcisol values without calcium carbonate are also contained within the vertisol range. The Fe_2O_3 in the calcisol is 7.1%-7.9%, while the vertisol is 5.2%-10.9%. The SiO_2 for vertisol is 52.5%-76.9%, while the calcisol has values of 62.5%-68.2% for SiO_2 if the $CaCO_3$ is factored out. This is a strong indicator that the parent material for the calcisol and

vertisol are from the same or similar sources, but prolonged weathering of the vertisol led to the dislocation of calcium while the calcisol developed in a calcium rich environment.

The clayeyness graph for the calcisol shows a strong increase up section (Fig. 13). This could be evidence for a increasing time of formation as the calcisol builds up, which would allow more clay to develop. It could also be evidence for a more diverse input through aeolian sources. The base loss graph jumps at 6.6 meters, possibly indicating more weathering at the top of the sequence (Fig. 13).

The calcification graph for the calcisol shows no trend through the section, though it does have wide variability (Fig. 13). The lack of trend and high variability are similarly mirrored on the base loss graph, which is an accumulation of insoluble products. The calcification and base loss data sets demonstrate inverse trends. For example, the highest amount of base loss in the calcisol corresponds with the lowest amount of calcification. This data trend represents the fluctuations between caliche nodule domination and the surrounding clay signal in sampling location. The scale at which these two trends occur is very different due to the high percentage of calcium within the caliche. High base loss and low calcification could be an indicator of weathering at time of deposition or slowing deposition.

There is little evidence for dolomitization in the calcisol formation because the MgO amounts are negligible relative to CaO (Table 1). Salinitization remains within a constant range throughout the caliche section (Fig. 13).

Compaction of paleosols

The basin is filled with up to 3 km of sediment (Barbeau, 2003). Current stratigraphic measurements of the section show 1200 meters of the fill remain in the area,

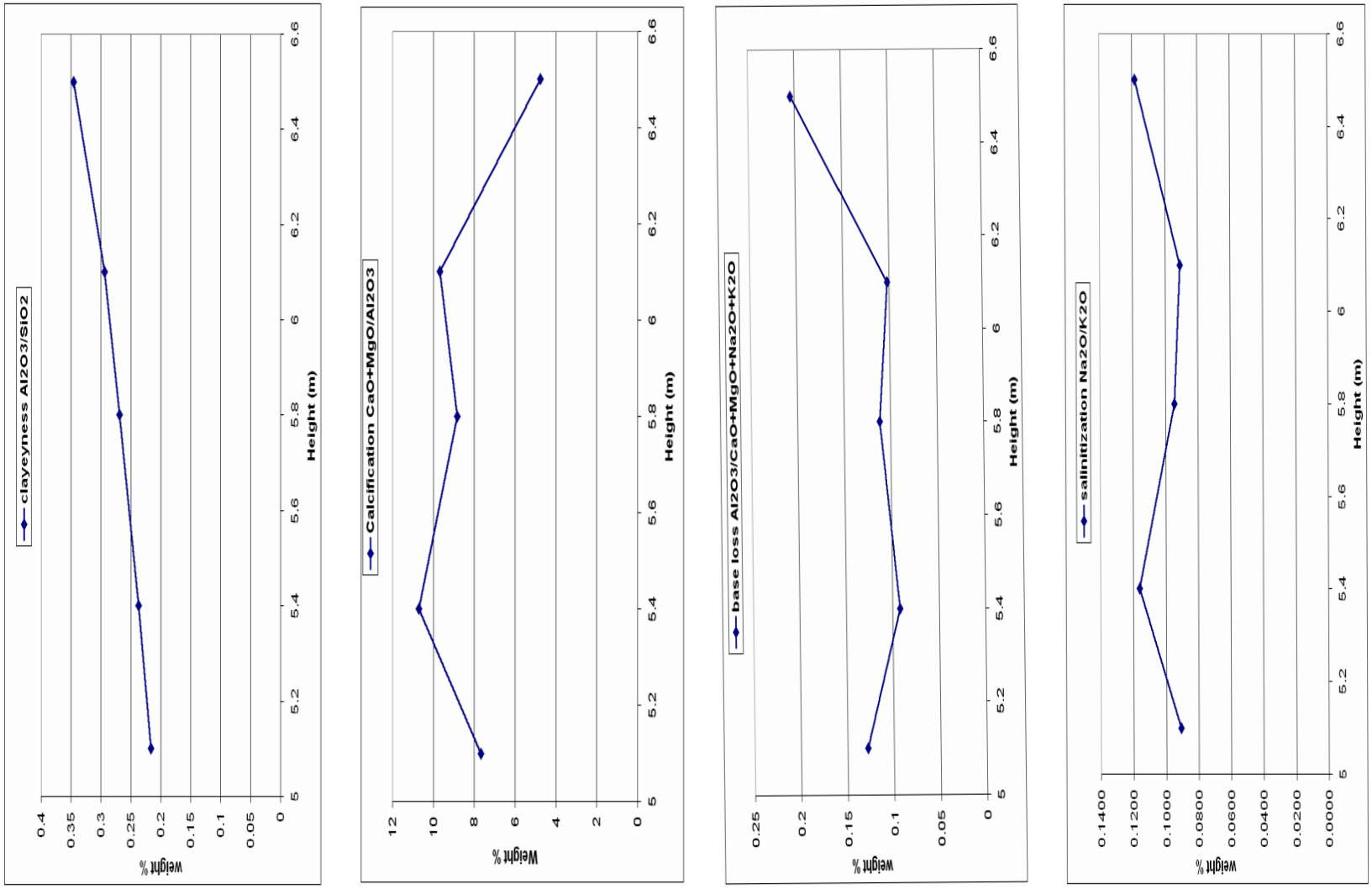

Figure 13: calcisol data. Relationships from Retallack (1997), showing clayeyness (Al_2O_3/SiO_2), calcification ($CaO+MgO/Al_2O_3$), base loss ($Al_2O_3/CaO+Na_2O+K_2O$) and salinitization (Na_2O/K_2O).

but since erosional approximations are unconstrained, estimates for the burial of the paleosols will be calculated with 3km of burial.

For the vertisol, a vertic-calibrated equation from Caudill et al. 1997 is given as:

$$C = -0.70/[0.49/(e^{(D/3.7)})-1]$$

where C is compaction and D is depth of burial in km (Caudill et al., 1997).

For 3km of burial, the compaction is 93% of original thickness. The vertisol is currently 6m, so its original height was 6.45m.

A paleosol compaction equation is developed by Sheldon and Retallack (2001), in which the original densities and material porosities are taken under consideration. Their favored compaction equation is:

$$C = -S_i/[(F_o/e^{Dk})-1]$$

where C is compaction, D is depth of burial in km, and the other variables are dependant on the soil types (Sheldon and Retallack, 2001). S_i is initial solidity, F_o is initial porosity and k is a constant (Sheldon and Retallack, 2001). The calcisol paleosol is most similar to the Retallack (1997) categorization of aridisol. This makes the $S_i = 0.62$, $F_o = .038$ and $k = 0.17$ (Sheldon and Retallack, 2001). For 3 km of burial, the compression is 80% of original thickness. The calcisol is currently 3.85m high, so originally it was 4.81 m before compaction.

The fresh water carbonate is measured at 1.5 meters. Because the porosity of the original material is unknown, the amount of compaction is undeterminable with any accuracy. The gypsisol differed in height depending on which side was measured, so compaction was also not considered due to lack of accuracy.

Timeline for development

Only a very broad estimate can be made about the amount of time the paleosol sequence represents, however an estimate can contribute in determining constraints in basin development. Due to abrupt transitions between paleosols, it is highly likely that time is lost to unconformities, which this estimate is unable to account for. The general rule of soil formation is that it takes 40 years per centimeter to form soil (Buol et al., 2003). An estimate contends that vertisols can form in 1000-5000 years, because they require so little pedogenesis that relatively quick formation could occur under suitable conditions (Birkeland, 1999). In warm, humid climates maximum time of formation is listed as less than 40,000 years (Nordt et al., 2004).

The estimates above do not take the elevation into account. Also, vertisols experience greater weathering in humid climates in comparison to arid to semiarid climates (Nordt et al., 2004). This would allow for a shorter development time. The uncompressed vertisol stands at 6.45 meters. To choose the middle ground from estimates ranging from 1000-40,000 years, while accounting for the great height, a rough estimate of 25,000 of development for the vertisol is given, which coincides with the Boul et al. (2003) estimate of 25,800 years based on height rather than soil material.

Precipitation rates of freshwater carbonates on pre-existing limestone have been cited as up to 2.2mm per year (Merz-Preiss and Riding, 1999). Rates for tufa freshwater carbonate deposition are highly variable, ranging from less than 1mm per year to circa 50 cm per year (Viles and Goudie, 1990). Half of the estimates in the Viles and Goudie (1990) review are under 1mm growth rate per year. Due to the lack of consensus, an

estimate of 1mm per year will be used, therefore allowing the formation of the tufa to occur in 1500 years.

Soil calcification generally occurs in areas with a low rate of sedimentation (Hubert, 1977). Calcrete and caliche formation time in poorly drained areas is estimated at 1000 years per meter (Meyer, 1997). With 4.81m meters of caliche before compaction, the estimated time of formation for the paleosol is 4810 years.

For the gypsisol body until the marl was reached (the length depicted in Figure 4 column B), 40yr/cm will be used for a rough temporal estimate, giving us a value of 62,600 years (Buol et al., 2003). This is likely an underestimate because compaction was not taken into consideration due to the poorly defined boundaries of the gypsum body.

Based on these estimates, the minimum total time of development is 100,000 years for just the paleosols, not accounting for additional marls on top of the sequence. If unexposed intervals of the section and the marl are accounted for using the measurements of Barbeau et al. (2005) then the section would be 100m high. Using an estimate of 0.1m per thousand years (m/kyr) for maximum alluvial plain paleosol formation, the section would total approximately 1 million years for the upper limit on development time (Behrenmeyer et al., 1995). Unconformities within the section could raise the time to be greater than 1 million years, as forebulges are generally considered areas of little to no deposition (DeCelles and Giles, 1996). The fluvial facies sedimentation rate above the paleosols and marl is estimated to average about 0.11m/kyr (Swanson-Hysell, 2005).

Discussion

Climatic Implications

Vertisols can form in a broad range of climatic environments. Precipitation ranges from 250-3000mm annually, while mean average temperatures range from 9°C to 25°C (Robinson, 2002). On average, vertisols experience climatic conditions between 500-1000mm annual rainfall, and 15.5°C -16.5°C mean annual temperatures (Robinson, 2002). While vertisols can occur in a diverse set of climatic conditions, about 90% of all vertisols form in dry, tropical to subtropical environments, notably 70% in the semiarid tropics (Caudill et al., 1996).

The high whole rock percentages of aluminum and iron within the vertisol are indicators of tropical environment, as abundant heat and moisture would weather away other elements, notably $CaCO_3$. Excess Al^{3+} and Fe^{3+} are characteristic of laterite soil, depending on which definition is used to define iron and aluminum enriched paleosols (Meyer, 1997). Laterite is a buildup of weathering products, generally in a tropical zone, and appears red in color (Meyer, 1997). The vertisol has characteristically red to purple coloring and high percentages of insoluble elements indicate a more tropical and humid environment; however, the presence of the upsection calcisol is uncharacteristic of a tropical environment. Tufas appear in climates ranging from warm and semi-arid to temperate, and therefore it's presence is generally not constrained as a climatic indicator (Pedley et al., 1996).

The caliche of the calcisol forms in climates ranging from Mediterranean to arid (Meyer, 1997). The amassing of calcium carbonate in soil reflects a water deficit, making the condition of formation one in which low rainfall and high evaporation occur

(Strong et al., 1992). Modern calcretes are found in areas with mean annual temperature of 16°C-20°C (Allen, 1974; Strong et al., 1992). Seasonal rainfall for calcisols is generally between 100-500mm (Allen, 1974; Hubert, 1977).

Strong et al. (1992) noted that paleo-calcretes from aeolian sources with rhizocretions are believed to have formed in arid to semi-arid environments, but that the rhizocretion fabric was missing in more humid climates. This suggests that the calcisol formed in an arid climate. Presence of gypsum in soil is a broad indicator of a mean annual precipitation of less than 300mm (Retallack, 1994).

In modern settings, vertisols and calcisols can both form in an environment of approximately 16°C mean annual temperature and 500mm annual rainfall. However, this overlap is based on endpoint data of the two environments, which makes it an improbable scenario. Without evidence for another mechanism causing transition from vertisol composition to calcisol deposition, some type of environmental factor is an enticing option. The paleosol sequence could indicate a transition from humid and tropical to semi-arid conditions; the lower vertisol and tufa form in a more tropical environment, then the landscape becomes more arid during calcisol and gypsisol deposition.

The shift from more moist vertisols and tufas to drier calcisols and gypsisols could be an indicator of the Paleocene-Eocene transition, or the Eocene-Oligocene boundary. The Paleocene-Eocene is a time of global warming around 55 million years ago; while the Eocene-Oligocene boundary is associated with a glaciation about 34 million years ago. The evidence within the paleosol sequence is less suggestive of a temperature change, and more indicative of decreasing precipitation that could be forced

through changing temperatures. The paleosol area could thus have become more arid from a previously humid state.

The Paleocene-Eocene thermal maximum evidence indicates that high latitude surface and deep oceans rose between 6°C and 8°C (Crouch et al., 2003; Schmitz et al., 2001). The ultimate reason for the Paleocene-Eocene thermal maximum remains unknown (Bowen et al., 2004). The Paleocene-Eocene thermal maximum occurred over approximately 60,000 years and is hypothesized to occur from release of sea-floor methane hydrate reserves (Bolle et al., 2000; Bowen et al., 2004).

The Paleocene-Eocene thermal maximum is believed to document a climatic and hydrological change in the Iberian region towards a seasonally drier climate (Schmitz et al., 2001). The broad Tethys region (the modern Mediterranean between the Early Jurassic and Oligocene) was experiencing a warm and humid climate during the early Paleocene, which turned to an arid and warm climate during the Paleocene-Eocene transition (Bolle et al., 1999). Increasing evaporation from rising temperatures at the Paleocene-Eocene boundary in the Tethys region is believed to have caused an increase in poleward moisture transport in the atmosphere, leaving Iberia arid (Lu et al., 1998).

The Paleocene-Eocene thermal maximum is coupled with an amplified humidity gradient, causing hotter and drier summers (Schmitz and Pujalte, 2003). The southward paleolatitude of Spain could allow it to experience an evaporation alteration from the warming of the Paleocene-Eocene thermal maximum, which would enhance evaporation in the subtropics, resulting in increased moisture at high latitudes (Schmitz et al., 2001). The Paleocene-Eocene is also associated with a sea-level fall (Schmitz et al., 2001). This could lead to increased exposure of marine limestone, allowing an increase in calcium

available for calcisol development. Increased erosion of siliciclastic materials into the ocean during the thermal maximum is believed to occur from the loss of vegetation cover during the drying of Spain (Schmitz et al., 2001).

During the Mesozoic and Paleocene, the Iberian microcontinent is believed to have been tropical, allowing the development of kaolinite (Schmitz et al., 2001). The Tethys region experienced warm humid weather during the Late Paleocene, which favored intensive leaching of parent materials, which corresponds well to the vertisol section (Bolle and Adatte, 2001). The kaolinite which developed on Iberia during the tropical regime was eroded during the Paleocene-Eocene boundary aridation, and is found in ocean sediments around the Iberian peninsula (Schmitz et al., 2001). The influx of kaolinite in sediments is followed by high clay compositions of smectite, palygorskite and sepiolite, which are characteristic of arid climatic regimes (Bolle and Adatte, 2001).

The Eocene-Oligocene boundary is a period of global cooling and Antarctic glaciation (Cavagnetto and Anadon, 1996). Marine oxygen isotope data shows a decrease in surface and deep water temperatures (Wolfe, 1992). Flora in France and other regions of Western Europe show a loss of tropical vegetation during the Eocene-Oligocene boundary (Collinson, 1992).

An alternative hypothesis to the paleosols representing the Paleocene-Eocene boundary suggests that the Eocene was a time of tropical rather than arid climate in the Ebro Basin (Barbera et al., 2001; Cavagnetto and Anadon, 1996). It is suggested that global cooling in the late Eocene shifted from early-middle Eocene humid and warm conditions in the Ebro Basin to a more wet-dry seasonality in the late Eocene-Early Oligocene (Barbera et al., 2001). Cooling in global temperatures would decrease

evaporation of the oceans and alter global precipitation patterns, which could also allow an aridation to occur. Extension of arid speciation occurs in North America, China and Russia during the Late Eocene to early Oligocene, a possible indicator for a worldwide decrease in the global hydrologic cycle with the onset of cooler temperatures (Leopold et al., 1992).

The Tethys regional climatic change during the Paleocene-Eocene boundary timing has not been site specific to the Ebro Basin. Paleomagnatic data in the basin suggests that the basin experienced most of its foreland basin growth during the late Eocene and Oligocene, as correlated through rodent fossils (Barbera et al., 2001; Jones et al., 2004). Since the paleosol is estimated to represent up to a million years, it would likely correspond to the Eocene-Oligocene climatic change if it is in harmony with the paleomagnetic data. The Paleocene-Eocene boundary was approximately 19 million years earlier, and if the paleomagnetic data is correct, the basin stratigraphy would have developed long after the Paleocene-Eocene thermal maximum unless significant time is lost in discontinuous sedimentation. Directly up section of the paleosols (around 400 meters), Early to Middle Oligocene rocks have been located through magnetic stratigaphy work on fluvial to alluvial fan conglomerate (Swanson-Hysell, 2005).

The Eocene-Oligocene boundary is documented as a decline in tropical flora and fauna, as the associated glaciation changed the environment to Savannah-woodland floral assemblages in the Ebro Basin (Barbera et al., 2001; Cavagnetto and Anadon, 1996). Middle Eocene (Bartonian) dated stratigraphy from the Ebro basin contain pollen from tropical to subtropical warm climates, suggestive of humid vegetation (Cavagnetto and Anadon, 1996). Tropical and humid conditions are reported in the northern Ebro Basin

during the middle Eocene (Bartonian) as reconstructed through microbialites, alluvial flood plains and hydromorphic paleosols (Lopez-Blanco et al., 2000). In the Ebro Basin, the late Eocene (Priabonian) demonstrates the beginning of the transition to savannah flora, with the Oligocene plants common characteristic being low humidity (Cavagnetto and Anadon, 1996). Change of rodent fauna occurred at the Eocene-Oligocene, as believed to be related to aridation and cooling of the Ebro Basin to reflect global glaciation (Barbera et al., 2001).

Localized weather patterns affected by uplift of the Catalan Coastal Range could also cause regional drying or aridity. Another alternative is that the changing tectonics of the area cause small scale paleoenvironment basin changes that mirror climatic changes (Saez et al., 2003). The paleosols represent a change that can be explained through climate altering from humid to arid as evidenced through the dramatic change in composition without any apparent change in parent material. The onset of the Paleocene-Eocene thermal maximum caused a drying in the Tethys region, while the Eocene-Oligocene boundary is also associated with a transition from tropical to more arid conditions. Further investigation into the timing of the development of the Ebro Basin will clarify which of the two boundaries, if not more localized conditions on a different time setting, are causing the significant composition difference in the paleosols.

Foreland basin system

In comparing basin stratigraphy to other locations in Spain, similar lithofacies appear in Armenteros et al. (1995) hypothesis for distal alluvial fan development. They find that alluvial fan source material causes clay-rich vertisol-like pedology at the bottom, with calcitic calcretes associated with episodic sedimentation typical of a semi-

arid alluvial fan (Armenteros et al., 1995). Armenteros et al. (1995) also finds an increase of gypsum further into the basin of their study area, which is hypothesized as saline mud flats and ephemeral lakes. This is similar to the Ebro Basin, where the gypsum saturates the local sequence above the calcisol and later there appear lacustrine marls. The distant alluvial fan source could be the Catalan Coastal Range, due to its proximity, or the Iberian or Pyrenean Ranges, which would allow for the infrequent presence of materials, complementary to the slow formation of soils. Dust could feed the area with iron and other elements not readily available from the erosion of nearby limestone (Sancho et al., 1992).

Comparing models of deposition, Evans and Welzenbach (2000) examine the evolution of freshwater tufas and paleosols in the Black Hills and Badlands of North America. Under a humid paleoclimate regime, groundwater flowed and precipitated tufas and lacustrine limestone (Evans and Welzenbach, 2000). In the Evans and Welzenbach (2000) scenario, uplift of the Black Hills provided the water with carbonate saturation and an elevated recharge area, while the Catalan Coastal Range could provide the tectonic uplift needed to source the tufa in the Ebro Basin. Short lived carbonate ponds were prevalent on the landscape, which could also precipitate the tufa and marl in the Ebro Basin paleosol sequence (Evans and Welzenbach, 2000).

The paleosol formation is likely to develop sluggishly, sourced from a slow feeding remote alluvial fan because of the large amount of time associated with soil growth. Twice the sequence was covered in fresh water, once for the freshwater limestone tufa formation, and later on to allow the lucustrine marl cap on the sequence. Both could occur in relatively small ponds or bodies of water.

Forebulge depositional environments are frequently characterized by unconformities, stratal thinning or no deposition (Fig. 2) (DeCelles and Giles, 1996). Furthermore, forebulges characterized by paleosol deposition are documented by Currie (1997). Forebulges range between ten and a few hundred meters in height, and are thought to span dozens to hundreds of kilometers (DeCelles and Giles, 1996). The Ebro Foreland Basin is constricted in size by competing mountain ranges, limiting forebulge size and confusing the dynamics. It is generally believed that the Pyrenees control the major loading of the Iberian Plate.

In the Ebro Basin location, the presence of a freshwater carbonate makes it questionable that the sequence developed on the forebulge, if the forebulge was a major topographic high-point. If the forebulge was relatively high (hundreds of meters) erosional materials could be coming off of the nearby forebulge, which would allow the vertisol, high in Al, Si and Fe oxides to be deposited on the backbulge. The erosional surface of a nearby forebulge would be a good source for providing parent material for the vertisol, which differs drastically from the bedrock because of the lack of calcium. This scenario would allow the concentration of iron and aluminum, which could be slowly feeding into the area as aeolian dust. A nearby forebulge could also function as a source for the clasts found in the tufa freshwater limestone. Because the sequence was under water twice, it is less likely to be a major topographic high unless the area experienced lots of hydrologic activity. A relatively little buldge would fit the depositional sequence well. The forebulge height remains undetermined.

Paleosols are suggested to be evidence of a period of little or no deposition in the area; possibly caused by less accommodation due to uplift (Currie, 1997). Forebulge

migration can occur from high sediment accumulation, causing the bulge to move away from the mountain range (White et al., 2002). If the forebulge were migrating from the Pyrenees southward, it could allow the field site to develop on lower topography, such as a backbulge. The backbulge setting would explain the freshwater pooling in the area. The Ebro Basin forebulge could move southward from the Pyrenees towards the site area. The eventual arrival of the forebulge would be an explanation for why the area is currently exposed. Alternatively, the vertisol could be deposited on the forebulge, where it experienced slow deposition and intense weathering. Migration of the forebulge over time could allow for underwater facies to develop later on, such as those seen in the marls and fluvial rocks.

In a third scenario, the elevation caused by the forebulge facilitated soil formation rather than a thicker, more sedimentary sequence sourced from alluvium. The area has remained on the forebulge throughout development, with regional ponds occurring on occasion in conjunction to changing climatic conditions. An active hydrologic setting could facilitate freshwater limestone and marl regardless of topographic height.

Conclusions

The Ebro Basin contains sediments that accumulated in a foreland basin of tectonic origin and begins with a paleosol sequence. The paleosols represent roughly 100,000 to 1 million years, though the time could be greater due to the abrupt changes in paleosols which are characteristic of unconformities. Paleoenvironment can be derived from the paleosols based on the following observations.

The vertisol and tufa formation are characteristic of humid climates, but the calcisol and gypsisol are evidence for more arid deposition. The change in paleosol composition can be explained as a transition from humid to arid environments in a warm climate. Climatic change provides a ressaon why two very different types of soils formed in the same area without evidence of a change in source material. The whole rock geochemistry shows that the vertisol and calcisol are similar in in aluminum, iron and silicon percentages when $CaCO_3$ is removed from the calcisol data, a indicator of similar parent material. In the more moist environment of the vertisol, increased vegetation in the tropical climate would allow for the reduction of sources of calcitic dust, while the humidity would cause increased weathering of the soil. As the area dried out, vegetation would die off and lakebeds would dry out; sourcing more calcium to the area and allowing for the deposition of the calcisol paleosol.

The aridification likely occurred at either the Paleocene-Eocene boundary, or the Eocene-Oligocene transition. The Tethys region of the Mediterranean during the Paleocene-Eocene thermal maximum shows a transition from tropical humid climate to more aridness through clay evidence in ocean sediments (Bolle and Adatte, 2001; Lu et al., 1998; Schmitz et al., 2001). Alternatively, the Eocene-Oligocene also shows a transformation from tropical to a more arid environment through changing floral and faunal assemblages in other Ebro Basin locations (Barbera et al., 2001; Cavagnetto and Anadon, 1996).

The paleosol sequence was deposited near or on the forebulge of the foreland basin, sourced mainly by distal alluvial fans and dust. The Pyrenees appear to be the major control of lithospheric flexure causing the forebulge; source material is likely

dominated by the Catalan Coastal Range. Soils represent slow deposition due to a sluggish input of material. With three nearby mountain ranges as source materials, it seems that the paleosols represent a relatively high rate of deposition compared to more traditional forebulge models.

Further investigations could utilize XRD analysis of clays increase support for the climatic change hypothesis. Improvement in the basin development timeline would also be helpful.

Acknowledgements

I would like to thank my two advisors; Dave Barbeau at University of South Carolina and Bereket Haileab at Carleton College. This project was funded in part by a Bernstein Endowment Research Grant and the Carleton College Geology Department. Ellen Schaal, Amy Moragues and Nick Swanson-Hysell assisted in the field. Kristin O'Connell provided a very helpful draft review, as well as Mike Bagley. Fruitful discussions with Mike Smith, Mary Savina, Phil Camill and Clint Cowen also assisted in this project's development. Lastly, the Prince of Horta, the College Street Co-op, an adult size tricycle, Rueb'n'Stein Happy Hour and the students of Carleton College made the process much more enjoyable.

References

Allen, J. R. L., 1974, Studies in fluviatile sedimentation: implications of pedogenic carbonate units, Lower Old Red Sandstone, Anglo-Welsh outcrop: Geological Journal, v. 9, no. 2, p. 181-208.

Armenteros, I., Bustillo, M. A. A., and Blanco, J. A., 1995, Pedogenic and groundwater processes in a closed Miocene basin (northern Spain): Sedimentary Geology, v. 99, p. 17-36.

Barbeau, D. L., 2003, Alluvial-fan architecture in thrust-belt growth strata: southwestern Catalan Coastal Ranges, Ebro basin, Spain. [Phd thesis]: University of Arizona.

Barbeau, D. L., Swanson-Hysell, N., Schaal, E., Stalker, K., DeCelles, P. G., Kirschvink, J., and Haileab, B., 2005, Kinematic Evolution of the Southern Ebro Foreland Basin, *in* AAPG Annual Convention Technical Program, Calgary.

Barbera, X., Cabrera, L., Marzo, M., Pares, J. M., and Agusti, J., 2001, A complete terrestrial Oligocene magnetobiostratigraphy from the Ebro Basin, Spain: Earth and Planetary Letters, v. 187, p. 1-16.

Behrenmeyer, A. K., Willis, B. J., and Quade, J., 1995, Floodplains and paleosols of Pakistan Neogene and Wyoming Paleogene deposits: a comparative study: Palaeogeography, Palaeoclimatology, Palaeocology, v. 115, p. 37-60.

Bestland, E. A., Retallack, G. J., Rice, A. E., and Mindszenty, A., 1996, Late Eocene detrital laterites in central Oregon: Mass balance geochemistry, depositional setting and landscape evolution: Geological Society of America Bulletin, v. 108, no. 3, p. 285-302.

Birkeland, P. W., 1999, Soils and Geomorphology: New York, Oxford University Press.

Bolle, M. P., and Adatte, T., 2001, Palaeocene-early Eocene climatic evolution in the Tethyan realm: clay mineral evidence: Clay Minerals, v. 36, p. 249-261.

Bolle, M. P., Adatte, T., Keller, G., Von Salis, K., and Burns, S., 1999, The Paleocene-Eocene transition in the southern Tethys (Tunisia): climatic and environmental fluctuations: Bulletin de la Societe Geologique de France, v. 170, no. 5, p. 661-680.

Bolle, M. P., Pardo, A., Adatte, T., Von Salis, K., and Burns, S., 2000, Climatic evolution on the southeastern margin of the Tethys (Negev, Israel) from the Palaeocene to the early Eocene: focus on the late Palaeocene thermal maximum: Journal of the Geological Society, v. 157, p. 929-941.

Bowen, G., Beerling, D., Koch, P., Zachos, J., and Quattlebaum, T., 2004, A humid climate state during the Palaeocene/Eocene thermal maximum: Nature, v. 432, p. 495-499.

Buol, S. W., Southard, R. J., Graham, R. C., and McDaniel, P. A., 2003, Soil Genesis and Classification: Ames, Iowa State Press.

Catalunya, I. C. d., 2003, Comarques de I'Ebre: I'Institut Cartografic de Catalunya.

Caudill, M. R., Driese, S. G., and Mora, C. I., 1996, Preservation of a paleo-vertisol and an estimate of Late Mississippian paleopercipitation: Journal of Sedimentary Research, v. 66, no. 1, p. 58-70.

-, 1997, Physical compaction of vertic palaeosols: implications for burial diagenesis and palaeo-precipitation estimates: Sedimentology, v. 44, p. 673-685.

Cavagnetto, C., and Anadon, P., 1996, Preliminary palynological data on floristic and climatic changes during the Middle Eocene-Early Oligocene of the eastern Ebro Basin, northeast Spain: Review of Paleobotany and Palynology, v. 92, p. 281-305.

Collinson, M., 1992, Vegetational and floristic changes around the Eocene/Oligocene boundary in Western and Central Europe, *in* Prothero, D. R., and Berggren, W. A., eds., Eocene-Oligocene Climatic and Biotic Evolution: Princeton, NJ, Princeton University Press.

Crouch, E. M., Dickens, G. R., Brinkhuis, H., Aubry, M.-P., Hollis, C. J., Rogers, K., and Visscher, H., 2003, The *Apectodinium* acme and terrestrial discharge during the Paleocene-Eocene thermal maximum: new palynological, geochemical and calcareous nannoplanton observations at Tawanui, New Zealand: Paleogeography, Paleoclimatology, Paleoecology, v. 194, p. 387-403.

Currie, B. S., 1997, Sequence stratigraphy of nonmarine Jurassic-Cretaceous rocks, central Cordilleran foreland-basin system: Geological Society of America Bulletin, v. 109, no. 9, p. 1206-1222.

DeCelles, P. G., and Giles, K. G., 1996, Foreland basin systems: Basin Research, v. 8, p. 105-123.

Delgado, R., Martin-Garcia, J. M., Oyonarte, C., and Delgado, G., 2003, Genesis of the terrae rossae of the Sierra Gador (Andalusia, Spain): European Journal of Soil Science, v. 54, p. 1-16.

Driese, S. G., Mora, C. I., Stiles, C. A., Joeckel, R. M., and Nordt, L. C., 2000, Mass-balance reconstruction of a modern Vertisol: implications for interpretating the geochemistry and burial alteration of paleo-Vertisols: Geoderma, v. 95, p. 179-204.

Elorza, M. G., and Santolalla, F. G., 1998, Geomorphology of the Tertiary gypsum formations in the Ebro Depression (Spain): Geoderma, v. 87, p. 1-29.

Evans, J. E., and Welzenbach, L. C., 2000, Lacustrine Limestones and Tufas in the Chadron Fromation (Late Eocene), Badlands of South Dakota, U.S.A., *in* Gierlowski-Kordesch, E. H., and Kelts, K. R., eds., Lake basins through space and time: AAPG Studies in Geology: Tulsa, OK, American Association of Petroleum Geologists, p. 349-358.

Glover, C., and Robertson, A., 2003, Origin of tufa (cold-water carbonate) and related terraces in the Antalya area, SW Turkey: Geological Journal, v. 38, p. 329-358.

Guimera, J., 1984, Palaeogene evolution of deformation in the northeastern Iberian Peninsula: Geological Magazine, v. 121, no. 5, p. 413-420.

Hubert, J. F., 1977, Paleosol caliche in the New Haven Arkose, Connecticut: Record of semiaridity in Late Triassic- Early Jurassic Time: Geology, v. 5, no. 5, p. 302-304.

Jones, M. A., Heller, P., Roca, E., Garces, M., and Cabrera, L., 2004, Time lag of syntectonic sedimentation across an alluvial basin: theory and example from the Ebro Basin, Spain: Basin Research, v. 16, p. 467-488.

Leopold, E., Lui, G., and Clay-Poole, S., 1992, Low-biomass vegetation in the Oligocene?, *in* Prothero, D. R., and Berggren, W. A., eds., Eocene-Oligocene Climatic and Biotic Evolution: Princeton, NJ, Princeton University Press, p. 399-420.

Lopez-Blanco, M., Marzo, M., Burbank, D. W., Verges, J., Roca, E., Anadon, P., and Pina, J., 2000, Tectonic and climatic controls on the development of foreland fan deltas: Montserrat and Sant Llorenc del Munt systems (Middle Eocene, Ebro Basin, NE Spain): Sedimentary Geology, v. 138, p. 17-39.

Lu, G., Adatte, T., Keller, G., and Ortiz, N., 1998, Abrupt climatic, oceanographic and ecological changes near the Paleocene-Eocene transition in the deep Tethys basin: The Alademilla section, southern Spain: Eclogae geologicae Helvetiae, v. 91, p. 293-306.

Mack, G. H., James, W. C., and Monger, H. C., 1993, Classification of Paleosols: Geological Society of America Bulletin, v. 105, no. 2, p. 129-136.

Merz-Preiss, M., and Riding, R., 1999, Cynobacterial tufa calcification in two freshwaer streams: ambient environment, chemical thresholds and biological processes: Sedimentary Geology, v. 126, p. 103-124.

Meyer, R., 1997, Paleoalterites and Paleosols: Brookfield, VT, A.A. Balkema Publishers.

Nordt, L. C., Wilding, L. P., Lynn, W. C., and Crawford, C. C., 2004, Vertisol genesis in a humid climate of the coastal plain of Texas, U.S.A.: Geoderma, v. 122, p. 83-102.

Pedley, M., Andrews, J., Ordonez, S., Garcia del Cura, M. A., Martin, J.-A. G., and Taylor, D., 1996, Does climate control to morphological fabric of freshwater carbonates? A comparative study of Holocene barrage tufas from Spain and Britain: Palaeogeography, Palaeoclimatology, Palaeocology, v. 121, p. 239-257.

Retallack, G. J., 1994, The Environmental Factor Approach to the Interpretation of Paleosols: Soil Science Society of America Special Publication, v. 33, no. Factors of Soil Formation: A Fiftieth Anniversary Retrospective, p. 31-64.

-, 1997, A Colour Guide to Paleosols: New York, John Wiley & Sons.

Robinson, A. C., 2002, A chronosequence study of modern vertisols and application to interpreting the time significance of Paleozoic paleovertisols [Master of Science thesis]: University of Tennessee, 177 p.

Saez, A., Ingles, M., Cabrera, L., and de las Heras, A., 2003, Tectonic-palaeoenvironment forcing of clay mineral assembalges in nonmarine settings: the Oligocene-Miocene As Pontes Basin (Spain): Sedimentary Geology, v. 159, p. 305-324.

Sancho, C., Melendez, A., Signes, M., and Bastida, J., 1992, Chemical and Mineralogical Characteristics of Pleistocene Caliche Deposits from the Central Ebro Basin, NE Spain: Clay Minerals, v. 27, p. 293-308.

Schmitz, B., and Pujalte, V., 2003, Sea-level, humidity, and land-erosion record across the initial Eocene thermal maximum from a continental-marine transect in northern Spain: Geology, v. 31, no. 8, p. 689-692.

Schmitz, B., Pujalte, V., and Nunez-Betelu, K., 2001, Climate and sea-level perturbations during the Initial Eocene Thermal Maximum: evidence from siliciclastic units in the Basque Basin (Ermua, Zumaia and Trabakua Pass), northern Spain: Palaeogeography, Palaeoclimatology, Palaeocology, v. 165, p. 299-320.

Sheldon, N. D., and Retallack, G. J., 2001, Equation for compaction of paleosols due to burial: Geology, v. 29, no. 3, p. 247-250.

Strong, G. E., Giles, J. R. A., and Wright, V. P., 1992, A Holocene calcrete from North Yorkshire, England: implications for interpreting palaeoclimates using calcretes: Sedimentology, v. 39, p. 333-347.

Swanson-Hysell, N., 2005, Mangetic Reversal Stratigraphy in the Ebro Basin, near Horta de San Juan, Spain [Bachlor of Arts thesis]: Carleton College.

Viles, H. A., and Goudie, A. S., 1990, Tufas, travertines and allied carbonate deposits: Progress in Physical Geography, v. 14, no. 1, p. 19-41.

White, T., Furlong, K., and Arthur, M., 2002, Forebulge migration in the Cretaceous Western Interior basin of the central United States: Basin Research, v. 14, p. 43-54.

Wolfe, J., 1992, Climatic, floristic and vegetation changes near the Eocene/Oligocene boundary in North America, *in* Prothero, D. R., and Berggren, W. A., eds., Eocene-Oligocene Climatic and Biotic Evolution: Princeton, NJ, Princeton University Press, p. 421-436.